

# Partitioning Quantum Chemistry Simulations with Clifford Circuits

Philipp Schleich,<sup>1, 2, 3</sup> Joseph Boen,<sup>4, 3</sup> Lukasz Cincio,<sup>3</sup> Abhinav Anand,<sup>5</sup> Jakob S. Kottmann,<sup>1, 5</sup> Sergei Tretiak,<sup>3, 6</sup> Pavel A. Dub,<sup>7</sup> and Alán Aspuru-Guzik<sup>5, 1, 8, 9, 2, 10, \*</sup>

<sup>1</sup>*Department of Computer Science, University of Toronto, Canada.*

<sup>2</sup>*Vector Institute for Artificial Intelligence, Toronto, Canada.*

<sup>3</sup>*Theoretical Division, Los Alamos National Laboratory, Los Alamos, NM, USA*

<sup>4</sup>*Department of Applied Mathematics & Statistics,  
Johns Hopkins University, Baltimore, MD, USA*

<sup>5</sup>*Chemical Physics Theory Group, Department of Chemistry, University of Toronto, Canada.*

<sup>6</sup>*Center for Integrated Nanotechnologies, Los Alamos National Laboratory, Los Alamos, NM, USA*

<sup>7</sup>*Chemistry Division, Los Alamos National Laboratory, Los Alamos, NM, USA*

<sup>8</sup>*Department of Chemical Engineering and Applied Chemistry, University of Toronto, Canada.*

<sup>9</sup>*Department of Materials Science and Engineering, University of Toronto, Canada.*

<sup>10</sup>*Canadian Institute for Advanced Research (CIFAR) Lebovic Fellow, Toronto, Canada.*

Current quantum computing hardware is restricted by the availability of only few, noisy qubits which limits the investigation of larger, more complex molecules in quantum chemistry calculations on quantum computers in the near-term. In this work, we investigate the limits of their classical and near-classical treatment while staying within the framework of quantum circuits and the variational quantum eigensolver. To this end, we consider naive and physically motivated, classically efficient product ansatz for the parametrized wavefunction adapting the separable pair ansatz form. We combine it with post-treatment to account for interactions between subsystems originating from this ansatz. The classical treatment is given by another quantum circuit that has support between the enforced subsystems and is folded into the Hamiltonian. To avoid an exponential increase in the number of Hamiltonian terms, the entangling operations are constructed from purely Clifford or near-Clifford circuits. While Clifford circuits can be simulated efficiently classically, they are not universal. In order to account for missing expressibility, near-Clifford circuits with only few, selected non-Clifford gates are employed. The exact circuit structure to achieve this objective is molecule-dependent and is constructed using simulated annealing and genetic algorithms. We demonstrate our approach on a set of molecules of interest and investigate the extent of our methodology's reach. Empirical validation of our approach using numerical simulations shows a reduction of the qubit count of up to a 50% at a similar accuracy as compared to the separable-pair ansatz.

## I. INTRODUCTION

An important goal of computational chemistry is to understand the behavior of strongly correlated electronic systems, as they are relevant to many applications in materials science, for example, developing more efficient catalysts, drugs or high-temperature superconductors. Since the computational complexity of many existing classical numerical methods scales exponentially with system size owing to solving the Schrödinger equation, there has been increased interest in developing quantum algorithms for this task in recent years [1–3]. One of the most popular approaches for finding ground state [4] and several low-lying excited states [5–8] is the Variational Quantum Eigensolver (VQE) [9–11].

The VQE is a hybrid quantum-classical algorithm that utilizes the variational principle to find variational approximations to the eigenstates and associated eigenvalues of a molecular Hamiltonian. Given a molecular Hamiltonian encoded as a linear combination of tensor products of Pauli operators, the VQE utilizes a parameterized quantum circuit (PQC) to prepare a trial wavefunction (ansatz) and compute its energy. By optimizing

the parameters of the quantum circuit, approximations to the ground and also excited states and their energies can be obtained. The VQE has been successfully applied to simulations of small molecules on quantum hardware [12]. One strategy to find trial wavefunctions is given by chemically-inspired ansatze, such as the popular family of Unitary Coupled Cluster (UCC) ansatze [4, 13]. UCC utilizes domain knowledge from quantum chemistry to prepare trial wavefunctions by exciting electrons from a reference state, which is usually the Hartree-Fock state. In contrast, hardware-efficient ansatze [12, 14] construct circuits from a limited set of gates that exploit the characteristics of the underlying device, such as connectivity or coherence time. Instead of directly encoding chemical knowledge into the ansatz, hardware-efficient ansatze rather try to be maximally expressible given hardware constraints. Despite continuous development of quantum hardware, current devices are prone to significant errors and can only support a limited number of operations on a few qubits, which limits the complexity of the quantum circuits used to generate trial wavefunctions. Thus, the development of techniques for designing shallow and resource-efficient ansatze is not only academically significant, but also of considerable practical importance. High gate errors and low coherence times of devices that are available in the current and near future – so called

\* [aspuru@utoronto.ca](mailto:aspuru@utoronto.ca)

noisy intermediate-scale quantum computers (NISQ) [15] – pose a critical limit to the circuit depth. As a result, many techniques have been developed to find suitable shallow circuits, see Refs. [9, 11, 13] for a representative overview.

In this work, we attempt to clusterize circuits to facilitate the usage of existing NISQ devices to run larger experiments. There has been recent work in this direction, as in Refs. [16, 17]. Both studies attempt to discover clusters or reduce the number of qubits per circuit through the utilization of correlation metrics. While Ref. [16] makes use of mutual information to clusterize the circuit, Ref. [17] uses entanglement forging to divide the circuit into two pieces that are executed separately. In our method, we pre-define the clusters and generally “cut” the circuit into two equally large pieces. We consider two options in choosing the clusters. For a physically motivated choice, we use the separated-pair-ansatz from Ref. [18], which is classically tractable and provides a natural clustering into electron-pairs, which is found throughout generation of so-called pair-natural orbitals [19, 20]. Beyond that, we also consider arbitrary clusters. Here, we expect that the sub-optimal choice of clusters can be accounted for by the Clifford circuit since permutation of qubits can be realized as a sequence of Clifford gates. Then, to re-gain lost correlation by assuming the product state, we search for a re-entangling circuit. In order to enable that the quantum computation can be carried out on hardware with less number of qubits, we use this circuit for a similarity-transform with the circuit unitary (often called “fold” or “dress” in the literature) the Hamiltonian, [21] similar to virtual “Heisenberg circuits” as in Ref. [22]. The circuit that modifies the Hamiltonian is trained together with VQE circuits by minimizing the overall energy. This means that the (near-)Clifford circuit modifies the Hamiltonian so that its ground state is closer to a product state. This procedure is briefly outlined in Fig. 1. We emphasize here, that both the cluster circuits as well as the virtual circuits are to be optimized; this means that for each modification of the virtual circuit, the parameters in the cluster circuits will be adjusted.

For the re-entangling circuits, we will first focus on using Clifford circuits only. The latter describe sequences of unitaries composed of elements of the Clifford group. Thus, they leave the number of Pauli strings when transforming a Hamiltonian in the Pauli basis invariant. As a consequence, the measurement complexity does not increase as opposed to folding general gates into the Hamiltonian. This will be extended by near-Clifford circuits, which introduce a small number of non-Clifford operations into these gate sequences so that the expressibility is increased but the operator complexity does not increase vastly. It is known that Clifford circuits are efficiently simulatable classically but do not form a universal set of quantum gates [23–25]. Recognized early within the stabilizer formalism for quantum error correction [23], they have since garnered considerable attention for their

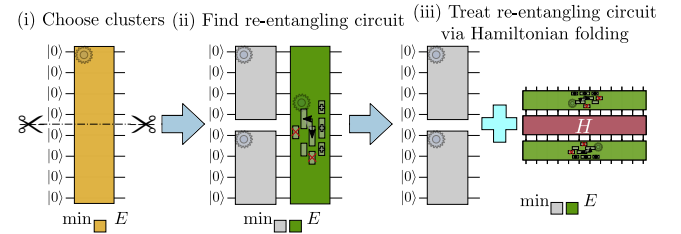


FIG. 1: Overview of our proposed method of dividing large system into smaller pieces. The ansatz consists of two parts: (i) VQE-like circuits denoted by gray boxes and with continuous, variational parameters (ii) near-Clifford, classically simulable circuit (green box) whose architecture is to be found by the optimizer as well. Near-Clifford circuits are evaluated by modifying (or dressing) the Hamiltonian  $H$ .

applications in other areas of quantum computing. For example, they have been proposed as an efficient and scalable way to perform random benchmarking of both near-term and fault-tolerant quantum computers [26–29]. As a scalable method for error mitigation [30], initialization strategies were developed to find better initial circuits and guesses for gate parameters based on Clifford gates only [29, 31]. Other areas of application include classically efficient compression of quantum circuits [32] and a standalone ansatz for variational quantum algorithms [33]. That ansatz however, is not able to reproduce the results obtained with universal gate sets due to limited expressibility of the Clifford group. In this study, we are exploring the limit to which classical post-processing (mostly relying on Clifford gates) can reduce the resource requirements in quantum chemistry calculations. Since Clifford gates form a discrete set, the optimization requires specialized techniques, described in Section II D.

We start this work by outlining our proposed methodology in Section II, including a motivation for the choice of clusters, looking at how to fold important circuit identities and the way Clifford and near-Clifford circuits are constructed. Then, we show results for simulating the ground-states of several molecules ( $H_2$ ,  $N_2$  and  $BeH_2$ ) in Section III before concluding our work in Section IV.

## II. METHODOLOGY

### A. Outline

In a VQE calculation, one aims to find an approximation  $E$  to the ground-state energy  $E_0$

$$E_0 \leq E = \min_{\psi} \langle \psi | H | \psi \rangle. \quad (1)$$

The state  $|\psi\rangle$  is usually prepared and optimized using a parametrized unitary operation  $|\psi(\theta)\rangle = U(\theta)|0\rangle$ , where  $U(\theta)$  acts on  $N_q$  qubits.

In this work, we prepare the wavefunction  $|\psi(\theta)\rangle$  through unitaries  $U_j(\theta_j)$  that only have local support on qubit-cluster  $j$  (cluster-local) followed by a global operation  $M(\tau)$  that is built using a (near-)Clifford circuit, which add some additional variational parameters  $\tau$ :

$$|\psi(\theta, \tau)\rangle = M(\tau) \prod_{j=1}^{N_{\text{cl}}} \underbrace{U_j(\theta_j)}_{=:|\psi_j(\theta_j)\rangle} |0\rangle. \quad (2)$$

Here,  $M(\tau)$  acts on the full space over  $N_{\text{q}}$  qubits, while  $U_j$  act only on the respective clusters  $j = 1, \dots, N_{\text{cl}}$  with  $N_{\text{q}}^{[j]}$  qubits. This way, we have a set of  $N_{\text{cl}}$  factorized states that can be evaluated independently and are then re-combined with  $M(\tau)$ . This circuit  $M(\tau)$  will be folded into the Hamiltonian. Our method can be summarized as a Schrödinger evolution on a subsystems with a virtual Heisenberg circuit that alters the Hamiltonian so that its ground-state resembles a product state over the subsystems. We provide an outline of the procedure in comparison with the standard, Schrödinger-picture-like VQE, in Fig. 2.

In what follows, we will first discuss how one can choose the subsystems in Section II B. Then, as the main contribution of this work, we will outline our procedure to find the virtual circuit  $M(\tau)$  in Section II C so that one regains maximum correlation energy.

## B. Clustering into subsystems

We choose subsystems either in a naive, uninformed, or physically motivated manner.

In the naive approach, we set clusters by simply cutting the circuit in  $N_{\text{cl}}$  roughly equally large clusters without considering any additional information. This allows us to test the capabilities of the re-entangling circuit  $M(\tau)$  to correct shortcomings of the naive clustering compared to the physically motivated approach and experiment with more arbitrary clusterings - for example, within electron pairs. In particular, we will see that the inclusion of permutations [34] into the ansatz allows the approach to retrieve a more optimal clustering.

For the physically motivated splitting, we use the separated-pair ansatz (SPA) [18] with fixed pair-natural orbitals – i.e., we are not considering orbital-optimization as in [35]. The SPA ansatz admits a natural decomposition into factorized clusters made up by  $N_{\text{el}}/2$  electron pairs, where the full wavefunction reads (cp. Eq. (15) in Ref. [18])

$$|\psi_{\text{SPA}}\rangle = \prod_{j=1}^{N_{\text{el}}/2} U_j(\theta_j) U_{\text{HF}} |00 \dots 0\rangle, \quad (3)$$

with pair-specific UCC-circuits  $U_j$ , number of electrons  $N_{\text{el}}$  and a circuit to prepare the Hartree-Fock state  $U_{\text{HF}}$ .

The reasoning behind our method is that we, on one hand, would like to push the boundaries of the classically

efficient SPA-ansatz, but also, on the other hand, expect a self-assembly of clusters throughout our technique. The latter can be understood in the sense of the so-called permVQE [34], where qubits (or conversely, orbitals) are permuted in order to maximize mutual information leading to a reduction in circuit depth. Since permutations are Clifford operations, including them in the allowed set of operators for  $M(\tau)$  does not increase complexity of the Hamiltonian. This means that the sub-optimal choice of clusters here is correctable by the virtual circuit  $M(\tau)$ .

As we will discuss later in Section II C, any modification of the Hamiltonian beyond Clifford gates may increase its complexity in form of the number of independent terms in the Pauli basis significantly. While it is in general beneficial to use measurement reduction techniques to lighten the measurement load, it can particularly help here when non-Clifford gates in  $M(\tau)$  increase the measurement complexity. These procedures typically effectuate a grouping of the Hamiltonian terms by various means so that multiple terms can be measured simultaneously [36–41]. At this point, we note that most of the techniques find a unitary operation that is applied directly before measurement so that the grouping of terms can be achieved in a desired basis. This is the case in particular for the methodologies outlined in Refs. [40, 41] that suppress the cost to at most  $\mathcal{O}(N^2)$  measurements. Unfortunately, this unitary gate needs to be evaluated on the quantum hardware with support beyond clusters for the method to be effective, which is impractical when dividing the circuit in clusters with the objective to run each cluster on hardware independently. However, one can still make advantage of graph clique cover methods such as Ref. [38] and especially the approach proposed in Ref. [39], which can also compress the measurements into a number of partitions that is at best order of  $N^2$ .

## C. Recovering correlation by folding a Heisenberg-circuit

Here, we describe our approach to construct the re-entangling circuit  $M(\tau)$  as in Eq. (2), carried out as a virtual Heisenberg circuit in the spirit of Ref. [16]. We first start by taking a closer look at folding typical circuit building blocks, not necessarily Clifford, in a generator formalism before introducing a procedure to build  $M(\tau)$ . Hereafter, we use the expression “to fold” a unitary circuit  $U$  into a Hermitian operator  $H$  to indicate a mapping according to a similarity transformation  $H \xrightarrow{U} U^\dagger H U$ . We will be using either purely-Clifford or near-Clifford circuits, which contain a small number of non-Clifford, parametrized gates to increase expressibility [42] of the circuit.

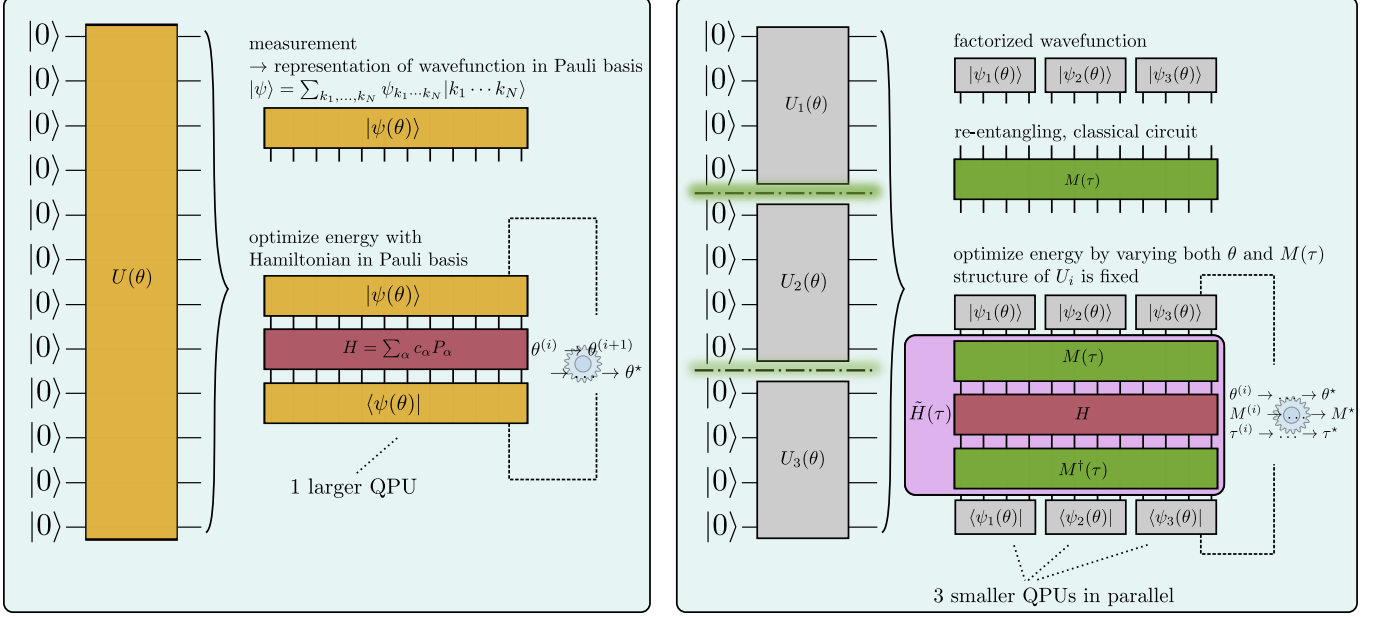


FIG. 2: Comparison of standard VQE procedure (left) and our approach (right), depicted using an example of three clusters.

### 1. Folding of important circuit identities

We aim to approximate the ground-state energy of an electronic system using an ansatz specified in Eq. (2) with a virtual circuit  $M(\tau)$ , given a clustering ansatz  $\prod_j U_j(\theta)$ . The resulting cost function, as in Eq. (1), then takes the form

$$\langle 0 | \left( \prod_{j=N_{\text{cl}}}^1 U_j^{\dagger}(\theta) \right) \underbrace{M(\tau)^{\dagger} H M(\tau)}_{=: \tilde{H}(\tau)} \left( \prod_{j=1}^{N_{\text{cl}}} U_j(\theta) \right) | 0 \rangle. \quad (4)$$

We consider virtual circuits that are built by a sequence of individual unitary gates  $M(\tau) = \prod_j V_j(\tau_j)$ , where individual operations can be expressed as

$$V_j(\tau_j) = \exp\left(-i\frac{\tau_j}{2} G_j\right) \quad (5)$$

for Hermitian generators  $G_j = G_j^{\dagger}$ . This allows us to implement the mapping  $H \xrightarrow{M(\tau)} \tilde{H}(\tau)$  by sequentially folding individual operations  $V_j(\tau_j)$ .

Since folding operations to find  $V_j^{\dagger} H V_j$  are an important part of our method (cp. to Fig. 2), we first look at efficient ways to find analytical implementations, using different classes of unitary gates. This encompasses recent work [43–46] related to analytical gradients for parametrized quantum circuits using the parameter-shift rule [47], where in this work, we resort to Refs. [43, 44] in particular. We first investigate rotation-like gates, whose generators are involutions, and gates that are generated by projections. Both have in common that their generators have exactly two eigenvalues, while the latter can be reformulated as the former by modifications so that

their spectrum is symmetric around zero. Beyond that, we discuss excitation-like gates, whose spectrum differs from involutions by an additional zero-eigenvalue, and discuss a strategy for general gates that is inspired by Ref. [44].

*a. Rotation-like gates.* For rotation-like gates such as  $R_X, R_Y, R_Z$ , the generators are involutions  $G^2 = \mathbb{1}$ . Hence we can write  $V(\tau) = \cos(\frac{\tau}{2})\mathbb{1} - i\sin(\frac{\tau}{2})G$ . This gives us the identity

$$\begin{aligned} \tilde{H}(\tau) &= \cos^2\left(\frac{\tau}{2}\right) H + \sin^2\left(\frac{\tau}{2}\right) GHG \\ &\quad - i\cos\left(\frac{\tau}{2}\right) \sin\left(\frac{\tau}{2}\right) [H, G]. \end{aligned} \quad (6)$$

*b. Projector-generated gates.* Another important class of gates is generated by projection operators, i.e.  $G^2 = G$ . We can motivate this class in the following way: If one tries to generate an  $X$ -gate by using the rotation  $R_X(\pi) = \exp(-i\frac{\pi}{2}X)$ , one obtains  $-iX$ . A phase-true  $X$  is generated by the projection  $G = \frac{1}{2}(\mathbb{1} - X)$  and  $\tau = 2\pi$ , i.e.  $X = \exp(-i\frac{\pi}{2}(1 - X))$ . One can thus generally relate this to the class of rotation-like gates from the above section with self-inverse generators  $\tilde{G}$  and associated angles  $\tilde{\tau}$  by setting  $\tau = 2\tilde{\tau}$  and  $G = \frac{1}{2}(\mathbb{1} - \tilde{G})$ :

$$V(\tau) = \exp\left(-i\frac{\tau}{2} G\right) \equiv \exp\left(-i\frac{\tilde{\tau}}{2} \tilde{G}\right). \quad (7)$$

This means that projector-generated gates are equivalent up to a  $U(1)$  transformation to rotation-like gates since  $\tilde{G}^2 = \mathbb{1}$ . We still deem it worthy to mention them as a separate class to emphasize that a phase-true implementation of certain gates requires a projection as generator,

which is of importance for controlled versions of these gates. Hence upon having done this substitution, the folding can be performed just as in Eq. (6).

*c. Excitation-like gates.* For quantum chemistry applications, circuit elements corresponding to fermionic excitations are of particular interest as they conserve particle-number symmetry. Beyond that, qubit excitations [13, 21, 48, 49] or (multi)-controlled rotations belong to this class. These gates belong to a class of operations that are generated by  $G = \mathbb{P}_+ - \mathbb{P}_- + \mathbb{P}_0$ , projecting on eigenstates with symmetric eigenvalues  $\pm\lambda$  and 0. One may express the generated unitary operator as [43]

$$V(\tau) = \cos\left(\frac{\tau}{2}\right)\mathbb{1} - i\sin\left(\frac{\tau}{2}\right)G + \left(1 - \cos\left(\frac{\tau}{2}\right)\right)\mathbb{P}_0. \quad (8)$$

The associated folded Hamiltonian is then

$$\tilde{H}(\tau) = \cos^2\left(\frac{\tau}{2}\right)H + \sin^2\left(\frac{\tau}{2}\right)GHG \quad (9)$$

$$\begin{aligned} &+ \left(1 - \cos\left(\frac{\tau}{2}\right)\right)^2 \mathbb{P}_0 H \mathbb{P}_0 \\ &- i\cos\left(\frac{\tau}{2}\right)\sin\left(\frac{\tau}{2}\right)[H, G] \quad (10) \\ &+ \cos\left(\frac{\tau}{2}\right)\left(1 - \cos\left(\frac{\tau}{2}\right)\right)\{H, \mathbb{P}_0\} \\ &+ i\sin\left(\frac{\tau}{2}\right)\left(1 - \cos\left(\frac{\tau}{2}\right)\right)(GH\mathbb{P}_0 - \mathbb{P}_0 HG). \quad (11) \end{aligned}$$

*d. General gates.* To obtain an exact expression for general gates, one can use the spectral decomposition of Hermitian generators  $G = \sum_k \lambda_k \mathbb{P}_k$ , with  $\lambda_k$  eigenvalues and  $\mathbb{P}_k$  projectors on the respective eigenspaces and then proceed similarly as for excitation-like gates, e.g. following the procedure outlined in section B.2. of Ref. [44]. If the dimensionality of the generator prohibits a numerical eigendecomposition, the gate may be decomposed into lower-dimensional building blocks.

*e. Hamiltonian-dependent identities.* Whenever the transformed Hamiltonian has specific properties they might be exploited for similarity transformations with specific gates. A prominent example relevant in the context of this work are fermionic single-excitations with  $G_{pq} = -i\kappa_{pq}a_p^\dagger a_q$  and anti-Hermitian matrix  $\kappa$  in combination with Hamiltonians consisting of fermionic annihilation (creation) operators  $a_p$  ( $a_p^\dagger$ ) only. Here, the operators are transformed as  $\tilde{a}_p^\dagger \equiv e^{iG}a_p e^{-iG} = \sum_q R_{pq}a_q^\dagger$  with the unitary matrix  $R = e^{-\kappa}$ . See the appendices of Ref. [35, 50] for details and applications, as well as Refs. [18, 51, 52].

## 2. Clifford circuits

We now have a recipe for folding different kinds of circuits. Next, we explore the types of circuits that facilitate the recovery of correlation energy lost through the clustering of states. Using quantum-chemical encoding

(see e.g. reviews [2, 3]), a molecular Hamiltonian can be written as a linear combination of Pauli strings

$$H = \sum_{\alpha} c_{\alpha} P_{\alpha} = \sum_{\alpha} c_{\alpha} \sigma_{\alpha_1} \otimes \cdots \otimes \sigma_{\alpha_{N_q}}, \quad (12)$$

where  $\alpha = (\alpha_1, \dots, \alpha_{N_q})$  and  $\sigma_{\alpha_j} \in \{\mathbb{1}, X, Y, Z\}$  is a Pauli matrix acting on site  $\alpha_j$ . We transform the original Hamiltonian as described in Section II C 1 and measure expectation value of

$$\tilde{H} = M(\tau)^\dagger H M(\tau) = \sum_{\alpha} c_{\alpha} M(\tau)^\dagger P_{\alpha} M(\tau). \quad (13)$$

The complexity of the measurement depends on the cardinality of the transformed Hamiltonian, i.e., the number of distinct Pauli strings in  $\tilde{H}$  that require independent measurement.

At this point, we notice that the cardinality of the transformed Hamiltonian can significantly grow, depending on the structure of  $M(\tau)$ . For single-qubit gates  $M(\tau) \in SU(2)$ , one can write

$$M(\tau) = \exp(i\tau \vec{n} \cdot \vec{\sigma}) = \cos(\tau)\mathbb{1} + i\sin(\tau)\vec{n} \cdot \vec{\sigma}, \quad (14)$$

where  $\|\vec{n}\| = 1$ ,  $\vec{\sigma} = (X, Y, Z)$ . We further note that the Pauli operators (together with phase factors, see Eq. (15)) form a group. On one qubit, this means that due to the closure property, transformation of a Pauli operator by a single-qubit operation as in Eq. (14) can only produce terms with  $\{\mathbb{1}, X, Y, Z\}$ , up to the phase factors. Thus for each single-qubit operator that transforms a Pauli-string in the Hamiltonian as in Eq. (12), the number of terms grows at most by a factor of 4. Then, for a system of  $N_q$  qubits, a virtual circuit consisting of only single-qubit gates leads to a cardinality of at most  $|\tilde{H}| \leq \mathcal{O}(4^{N_q}|H|)$  [53]. This bound holds as well for multi-qubit gates.

Thus, dressing the Hamiltonian with general gates is very costly and should be avoided. As an example, we show the increase in number of terms for folding a UCCSD circuit into the Hamiltonians for  $H_2$ ,  $BeH_2$  and  $N_2$  in Fig. 3. The cost-effective solution is given by gates from the Clifford group  $\mathcal{C}_n$ , which is defined as the subgroup of the unitary group that normalizes the Pauli group. That is, the set of unitary operations that keep the Pauli group

$$\begin{aligned} \Pi_n = \left\{ e^{i\theta \frac{\pi}{2}} \sigma_0 \otimes \cdots \otimes \sigma_n : \theta \in \{0, 1, 2, 3\}, \right. \\ \left. \sigma_j \in \{\mathbb{1}, X, Y, Z\} \right\} \end{aligned} \quad (15)$$

invariant under similarity transformations [54], i.e.

$$\mathcal{C}_n = \{U : U^\dagger \sigma U = \sigma'; \sigma, \sigma' \in \Pi_n\}. \quad (16)$$

Hence for  $M(\tau) \in \mathcal{C}_n$ , the cardinality of a Hamiltonian over  $n$  qubits remains unchanged.

However, for Clifford gates only, we just introduce a certain, restricted type of entanglement between the clusters as Clifford circuits are not universal [23, 55]. This

might already prove useful, but ultimately we consider *near-Clifford* circuits, so that we can control the additional cost and take benefit from more general transformations. Such circuits are composed mostly out of Clifford gates, however, also contain a limited number of non-Clifford gates in order to boost expressibility.

Ref. [56] also has investigated the growth of Hamiltonian terms for certain non-Clifford circuits as the qubit coupled cluster (QCC) approach can be formulated as a folding of the Hamiltonian. They found that, while exponential increase cannot be avoided, the coefficient  $c$  for an increase that goes as  $c^N$ , is smaller for so-called involutory linear combinations of entanglers that lead to a involution as opposed to standard QCC entanglers. More recently, Ref. [57] extended this work by exploiting the structure of the Clifford group to build a Hamiltonian that is folded by so-called normalizer Pauli strings rather than qubit excitations. Within their approach, they circumvent the complications that come with a discrete optimization problem, however, do not address a Clifford only circuit, which is the main focus of this work.

#### D. Optimizing Clifford circuits using a genetic algorithm

In this work, optimization refers to the process of minimizing the energy expectation value by optimizing the parameters in the circuits in the following sense: For the clusters  $U_j(\theta)$  with fixed architecture, the parameters  $\theta$  are varied. At the same time, both structure and parameters need to be adjusted for the near-Clifford circuits, which are supposed to account lost correlation due to the enforced product ansatz in the  $U_j$ 's. For the case when  $M \in \mathcal{C}_{N_q}$ , there are no continuous parameters available that would allow an adaptive scheme such as in the family of ADAPT-VQE methods [58, 59] and qubit coupled cluster techniques [21, 48] as the Clifford group only forms a discrete set. One could think of Bayesian mappings from the discrete gate set to a continuous parameter such as in Ref. [60] or a simple simulated annealing strategy as in Ref. [33]. In our tests, a simulated annealing strategy surpassed by a genetic algorithm, which is what we use and will describe in the following.

The genetic algorithm we choose resorts to an operator pool, which it uses as a reference set for the discrete optimization problem. Elements of the operator pool are used to modify the circuit by adding new operators and modifying existing gates in  $M(\tau)$ .

The operator pool we use can be found in Table I. Aside from the generators of the Clifford group ( $H, S, C_X$ ), we also include the Pauli gates, controlled Pauli gates, a SWAP gate to mimic permutations. These have proven helpful in Ref. [34] to reorganize the correlation pattern in the state, so it is easier to describe with a cluster product ansatz. We also include gate blueprints that are inspired by fermionic excitations [13], where we fix the angle of the freely parametrized  $R_Z$ -rotation in the center aim-

ing to obtain an approximate representation in form of a Clifford gate so that it is either one of  $S, Z, S^\dagger$ . These are supposed to mimic gate sequences that have proven useful in finding ground-states for quantum chemistry. Extending the gate pool may aid to speed up optimization, as these sequences can be picked from the pool and do not need to be found via optimization. Next, we explain the optimization procedure to find a Clifford circuit  $M$ , which is also described in Algorithm 1.

The general procedure to generate the classical circuit is outlined in Fig. 4. First, we generate a set of initial populations by randomly sampling circuits built from the operator pool. Any initial gates that do not have support over multiple clusters can be seen as an extension/modification of the cluster circuits; thus, one can choose to avoid them in the optimization procedure. We discuss this further in Section III C.

Based on the initial circuits per population, we impose a set of modifications, drawn randomly from the set of allowed operations. These are comprised of the addition of gates from the pool, exchanging specific gates with others or re-arranging them and deleting gates. We choose a scheduling so that each modification occurs with a certain probability; e.g., we found that favoring changing over deletion and addition is advantageous, while during early iterations the rate of additions should initially be higher.

---

#### Algorithm 1 Architecture search for $M$

---

```

1: Input operator pool, reference method / circuits, number
   of populations, offsprings per population and maximum
   iterations
2: for all populations do
3:   compute reference energy
4:   sample initial circuits  $M$ 
5:   optimize reference to compute energy with initial cir-
   cuits
6: end for
7: while not converged do
8:   for all populations do
9:     for all offsprings per population do
10:      propose modification to  $M$ 
11:      optimize reference to compute energy
12:    end for
13:    pick offspring to continue with based with proba-
       bility  $e^{-\frac{\Delta E}{T}}$ , update  $T$ 
14:  end for
15: end while
16: Output circuit  $M$ , optimal reference, approximation to
   ground-state energy

```

---

Then, for each population, we allow a number of offsprings/children with independent modifications. We pick the child with the lowest energy to continue the search. After a set number of iterations or when a convergence criterion is fulfilled – here, the change in energy between iterations – we end the optimization and pick the minimum over all populations as an approximation to the optimal solution. Within the search, we make use of an

Pool of Clifford gates  $\{H, S, X, Y, Z, C_X, C_Y, C_Z, \text{SWAP}, \text{Exc}_1, \text{Exc}_2\}$

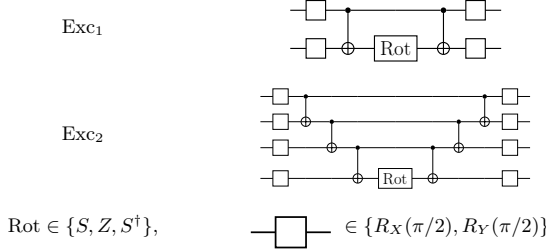


TABLE I: Operator pool used for Clifford optimization including excitation-like gates  $\text{Exc}_1, \text{Exc}_2$ . These consist of basis transformations, CNOT ladders and a central  $Z$ -rotation, which implements operations  $e^{-i\frac{\theta}{2}\sigma_1\sigma_2\cdots\sigma_N}$ , where the basis transformations allow  $\sigma_i$  to be any of  $\{X, Y, Z\}$ . Further,  $\text{Rot} \in \{S, Z, S^\dagger\}$ ,  $\theta \in \{\frac{\pi}{2}, \pi, \frac{3\pi}{2}\}$ .

additional “patience” hyperparameter – this parameter is increased whenever the modifications does not lead to an improvement in energy. When the patience parameter reaches a certain value, the associated population “frustrates” and re-sets its circuit instructions to a previous stage. We further allow updates such as in simulated annealing, where we pick the best offspring per population with probability  $e^{-\frac{\Delta E}{T}}$  and decrease temperature  $T$  over the course of iterations. As a result, the best improvement in energy is picked most likely but there is still a chance that even an increase in energy would be allowed to avoid local minima; however, we do not allow increases in energy beyond the minmum energy that was found for the employed reference method  $U$  with  $M = 1$ .

After each such optimization step, the parameters in the cluster circuit  $U_j(\theta)$  are adjusted. For the case of Clifford circuits, one may consider techniques proposed in Refs. [61, 62] to further optimize the depth of the resulting circuits.

### E. Near-Clifford circuits to increase expressibility

It is well-known that circuits made up from Clifford gates only are not universal [23]. We aim to counteract this by adding few non-Clifford gates to the circuit  $M(\tau)$ . However, we also know that including more and more non-Cliffords likely leads to an immense increase in number of terms in the Hamiltonian, making measurement intractable (cf. Section II C 2). Thus what we understand as a near-Clifford circuit is a circuit that results in a “reasonable” increase in the sense that  $|\tilde{H}| \leq C|H|$  for some moderately-sized constant  $C$ . In particular, we want to avoid a regime with exponential increase. An easy choice whose capabilities we will explore later on is modifying a single Clifford gate towards its parametrized version, i.e. for a Clifford gate  $U_{\text{Cliff}}$  with generator form  $U_{\text{Cliff}} = \exp(-i\theta_{\text{Cliff}}G)$  and fixed  $\theta_{\text{Cliff}}$ , we use  $U(\theta) = \exp(-i\theta G)$  with a free parameter that can be

used for optimization. Hence, for our experiments here, we will loop over all Clifford gates within the virtual circuits  $M$ , except for controlled gates and SWAP, and replace them with parametrized versions. We outline this strategy in Algorithm 2. For example, we substitute  $X \rightarrow R_X(\tau)$  or  $\text{Exc}_{1,2}$  (cp. with Tab. I) receive a  $R_Z(\tau)$  as center gate.

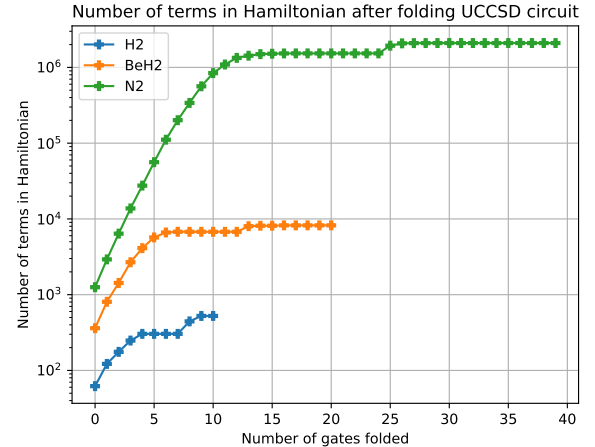


FIG. 3: Increase in number of terms in the Hamiltonian for  $\text{H}_2$ ,  $\text{BeH}_2$  and  $\text{N}_2$  molecules when folding a vanilla UCCSD circuit [13]. The horizontal lines without term increase correspond to Clifford gates.

---

### Algorithm 2 Optimization of near-Clifford $M(\tau)$ with one single-qubit non-Clifford gate

---

```

1: Input non-Clifford version of operator pool, reference
   method / circuits, optimized Clifford circuit  $M$  and maximum
   iterations
2: for all (single-qubit) Clifford gates  $V$  in  $M$  do
3:   replace  $V$  with its non-Clifford version  $g(\tau)$  and initial
   parameter set to correspond to Clifford
4:   while not converged do ▷ compute energy
5:     optimize reference
6:     optimize parameters in  $V(\tau)$  with only few iterations
7:   end while
8:   re-update reference and then  $\tau$  with smaller tolerance/more iterations
9: end for
10: set  $V(\tau)$  with best performance as non-Clifford
11: Output circuit  $M(\tau)$ , optimal parameter  $\tau^*$ , optimal reference and approximation to ground-state energy

```

---

## III. RESULTS

We will demonstrate our proposed technique on a set of small molecular examples to validate capabilities of Clifford and near-Clifford circuits to re-gain correlation due to the assumed product state. For the hydrogen

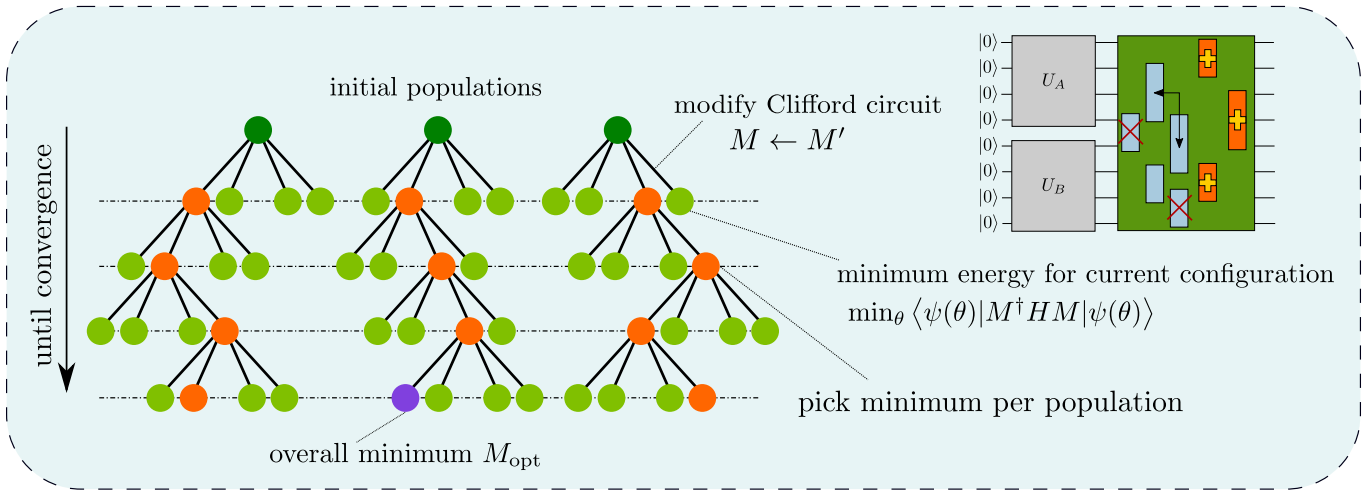


FIG. 4: Outline of the genetic algorithm used to assemble the classical circuit  $M$ . Based on some initial circuits (initial populations) made up by random gates drawn from the operator pool in Tab. I, random changes of this circuit in form of addition, deletion and change of gates as shown in the top-right corner, are proposed. The best change per circuit is used as a reference for the next iteration as long as this change does not perform worse than the reference method; this procedure is repeated until convergence or until a maximum number of iteration is reached.

molecule, we choose a basis set of Gaussians, whereas for beryllium hydride and the nitrogen molecule, we use a basis of pair-natural orbitals generated by multi-resolution analysis [18, 19], as described before.

We choose the following reference method for all our systems: We use a power method-type procedure that enforces a product state in the wavefunction to find the ground-state. A brief overview of this method can be found in appendix A.

### A. Simulation setup

Simulation code was written with the TEQUILA [63] framework using the QULACS simulator [64] as simulation backend for the quantum circuits and the automatically differentiable framework of [43]. Direct basis determination via pair-natural orbitals was performed with MADNESS [65] as described in Ref. [19] with the diagonal approximation described in Ref. [18] and the MP2-PNO implementation of Ref. [20] without cusp regularization. The latter interfaces mean-field implementations described in [66, 67]. Jordan-Wigner encoding corresponds to the implementation in OPENFERMION [68]. Orbitals in standard basis sets were computed with PSI4 [69].

For the genetic algorithm as outlined in Fig. 4, we choose the number of populations between 10–15 and the number of offsprings per population as 8–10. The convergence criterion for the reference method is set to  $10^{-5}$ , and the maximum number of iterations (tree depth in Fig. 4) is set between 10–25.

For all the following results, we show the error of various employed methods with respect to the exact ground

state (Full Configuration Interaction) within the same basis set. As a reference method, which produces and optimizes a product state via  $\prod_j U_j$ , we use a power method outlined in appendix A. With this as a starting point, we assemble a virtual circuit  $M$  built from Clifford gates only (“Reference + Cliffords”) and subsequently search over all Clifford gates and check if the energy can be improved by optimizing their parameter when making them parametrized (“Reference + Near-Clifford circuit”).

### Hydrogen molecule

We use the 6-31G basis set for  $\text{H}_2$ , where we choose an active space of six spin-orbitals to obtain a six-qubit toy example. As a reference, we enforce a product state of the “first” and “last” three orbitals, while first and last corresponds to the ordering with respect to orbital energies. As showcased in Fig. 5, this approach has a rather high error, of the order of hundreds of milli-Hartree. However, addition of a virtual Clifford circuit enables to suppress the error to the order of milli-Hartrees. In the case of small bond distances, the reduction is as much as three orders of magnitude. For large bond distances, the improvement by adding additional entanglement is lower but still accounts for roughly one order of magnitude. This is because the true state is close to a state preivable by a pure Clifford circuit supported only on the first four qubits as explained in Ref. [35]. To sum up, we observe significant improvement for Clifford-gates only. While the addition of freely parametrized non-Clifford gates does not reliably lower the energy, if successful, it can yield up to another order of magnitude in accuracy.

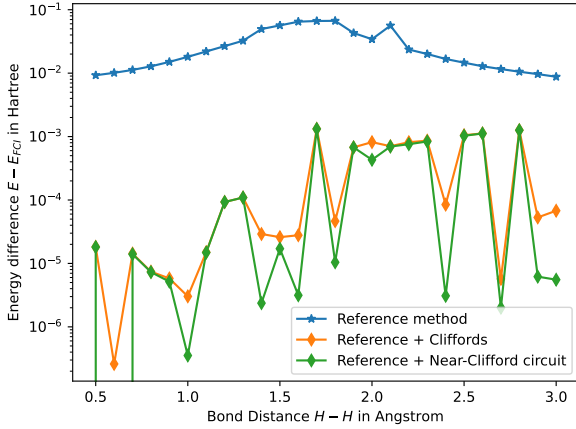


FIG. 5: Simulating the ground-state of  $\text{H}_2$  in the 6-31G basis set using an arbitrary active space of 6 qubits; here, we also use an uninformed clustering, where the first set of three and the second set of three qubits are enforced into a separable state.

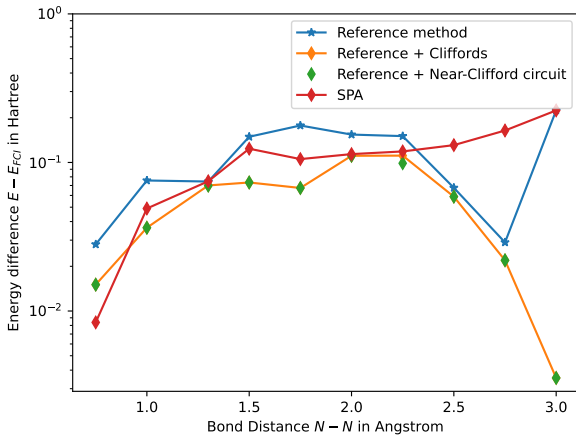


FIG. 6:  $\text{N}_2$  with two SPA pairs as clusters in frozen-core approximation, 12 qubit simulation

### Nitrogen molecule

For the  $\text{N}_2$  molecule (Fig. 6), the SPA outperforms our product state reference method in most regimes. However, for long bond distances, we can observe significant improvement. The SPA performs here due to the surrogate model that is used to generate the PNOs which are used as a basis. They are generated using second-order Møller-Plesset perturbation theory as a surrogate model and thus the PNOs inherit shortcomings of the surrogate model [19, 20, 70]. While our method makes use of the same PNO basis, it is, in contrast to the SPA, able to recover a part of this error.

Upon addition of a virtual Clifford circuit, we again observe a consistent improvement. It is noticeable that the SPA is still better for the lowest bond-length considered and that our method seems to perform better for short and large bond lengths. Furthermore, we found that parametrizing a single Clifford gate of the virtual circuit for the most part improves the energies compared to the Clifford circuit only barely. For this system, the genetic algorithm also showed rather unfavorable convergence behavior and tends to take very long time to achieve convergence.

### Beryllium hydride

We further consider  $\text{BeH}_2$  as a system of interest for comparability with results from Ref. [18]. We use a basis of eight qubits using MRA-PNOs (PNOs determined by multi-resolution analysis), made up by two clusters formed by two spatial orbitals based on each electron pair. As expected, we can see in Fig. 7a that the SPA-ansatz slightly outperforms our reference method. However, the addition of a virtual circuit made up by Cliffords only allows to improve beyond the SPA and this can be further boosted by parametrizing one of the Clifford gates. We further note that the improvement seems to produce a somewhat constant offset – the general behaviour of the error curve remains unchanged. This behaviour is similar to standard orbital optimization on top of the SPA reference (OO-SPA, as done in Ref. [18]). However, we note that the improvement by the found Clifford and especially near-Clifford circuits is generally slightly higher. This is despite that orbital optimizations are non-Clifford operations, but leave the complexity of the Hamiltonian unchanged. We observed that the behaviour of the procedure is more favorable if power method-based reference method is used instead of the SPA as a reference. The outcome of the initial optimization is somewhat randomized and therefore has eased to find gate sequences that lower the energy in subsequent iterations. Potentially, the SPA is stuck in a more stable local minimum than the iterative power-method based solver, which would make it harder to break free.

We next investigate the consequences of not utilizing the optimal clustering into electron pairs prior to the analysis. We mix pairs so that one spin-orbital of one pair is exchanged with one the other pair. Results for this case can be found in Fig. 7b as well as that the reference method behaves significantly worse. However, this does not seem to influence the outcome of the computations that include a virtual circuit. This is likely due to the inclusion of SWAP gates into the operator pool, which are able to retrieve the optimal clustering by permuting orbitals [34]. In fact, we notice here that the circuits built from Clifford gates only perform as well as the near-Clifford circuits for most geometries and performs slightly better as in the un-permuted case. Since the employed algorithm is random and the outcome of

the genetic algorithm with a finite number of populations and offsprings has some variance, this is not surprising.

### B. Increase in the number of Hamiltonian terms

For the results discussed above, we show the increase of the number of terms in the Hamiltonian when folding the classical circuit in Fig. 8. We show both the cardinality before ( $|H|$ ) and after folding ( $|\tilde{H}|$ ). Additionally we demonstrate the range of cardinalities that can be accessed by exchanging one Clifford gate for another one in the previously optimized Clifford circuits for each geometry. As expected, the upper bound of  $4^{N_q}$  times the previous complexity is respected.

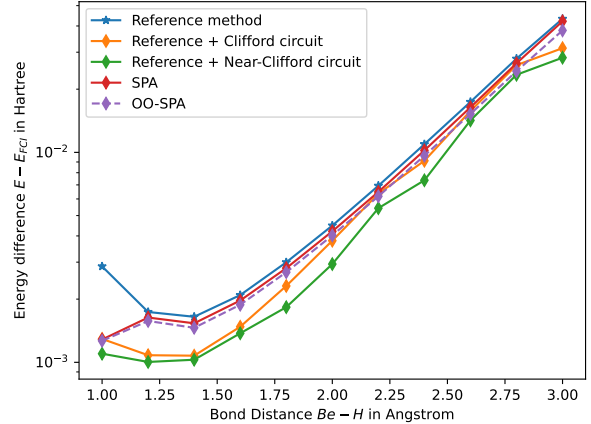
While it is clear that the measurement cost increases, we note that the increase when folding one gate should be manageable given that a single non-Clifford gate only increases the complexity by a constant factor. In fact, in the case of hydrogen,  $|\tilde{H}|$  at the optimized circuit is almost at the lower bound of the range of circuits. However, this cannot be established as a trend for the larger systems.

### C. Circuit structures

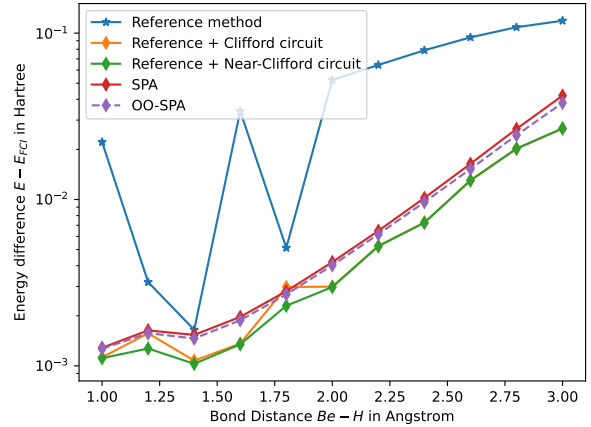
We further take a look at the characteristics of the learned circuits in order to check if there are some distinct circuit building blocks noticeable that have been favored by the genetic algorithm used. We note that a recurring theme in the circuits discovered are  $C_X$  ladder-like structures that entangle and exchange information across the qubits (Fig. 9). One can also see that in the way we set up the algorithm, there is an initial part of the circuit that does not have support beyond the clusters. This means one can see this section of the virtual circuit rather as a part of  $U$  than  $M(\tau)$ , and one may choose to not allow such gates if one assumes the reference circuit  $U$  is already good enough. An argument for leaving the gates that could be incorporated into the cluster-unitaries  $U_j$  is that the algorithm has identified a part of the description of the cluster-states  $|\psi_j\rangle$  that can be described classically. This is beneficial when an ansatz for the circuits  $U_j$  has been established that is evaluated on real quantum computer. Then, thanks to  $M$ , the circuit for  $U_j$  could be shorter.

## IV. CONCLUSION AND OUTLOOK

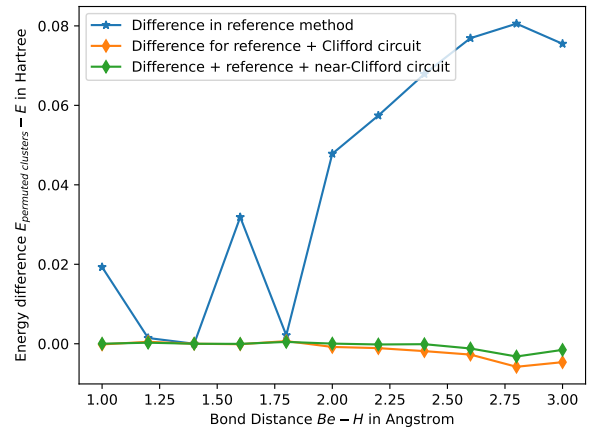
In this work, we investigate whether a larger quantum chemical simulation can be run on smaller quantum computers without sacrificing the accuracy too much. This procedure is of practical interest because it allows to make use of smaller quantum computers that will be available in the near future. Furthermore, reducing the circuit size can allow to alleviate the problem of limited



(a)  $\text{BeH}_2$  with clusters according to electron pairs, 8 qubit simulation



(b)  $\text{BeH}_2$  with permuted reference clusters, also see Fig. 7c.



(c) Comparison of  $\text{BeH}_2$  with pair-wise and modified clusters, showing energy difference between permuted clusters and clusters by electron pairs. For a configuration between clusters  $A$  and  $B$  as  $(000_A, 111_B)$ , where 0,1 shows association to an electron pair, we permute to  $(100_A, 011_B)$ .

FIG. 7: Errors of optimization results with respect to FCI in corresponding bases.

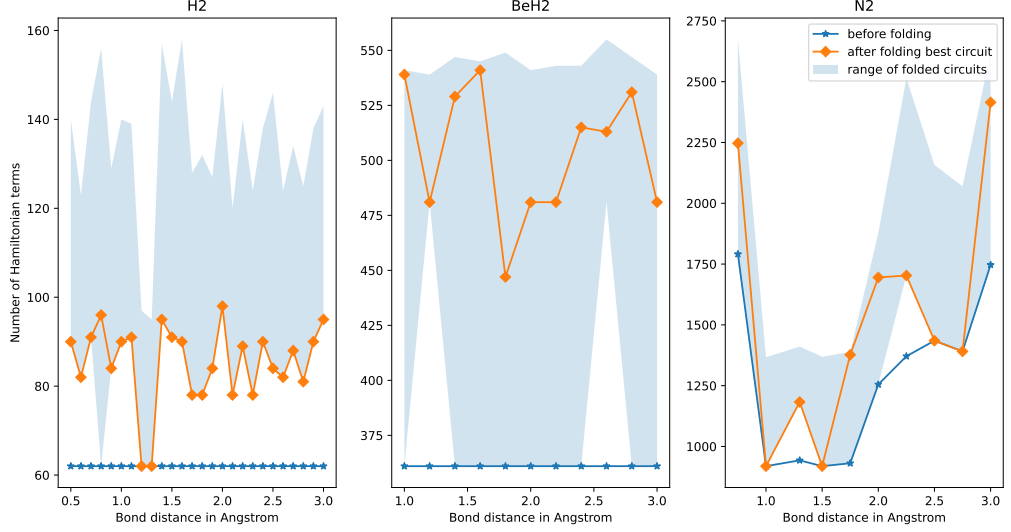


FIG. 8: Increase of the number of terms in the Hamiltonian after folding the optimized circuits when using only one gate of the circuit as a parametrized non-Clifford gate. The range of folded circuits depicts the envelope of maximum- and minimum number of terms that are possible when parametrizing a single gate of the previously optimized Clifford circuit, assuming the parametrization makes them non-Clifford. Otherwise the minimum coincides with the number of terms before folding (blue line).

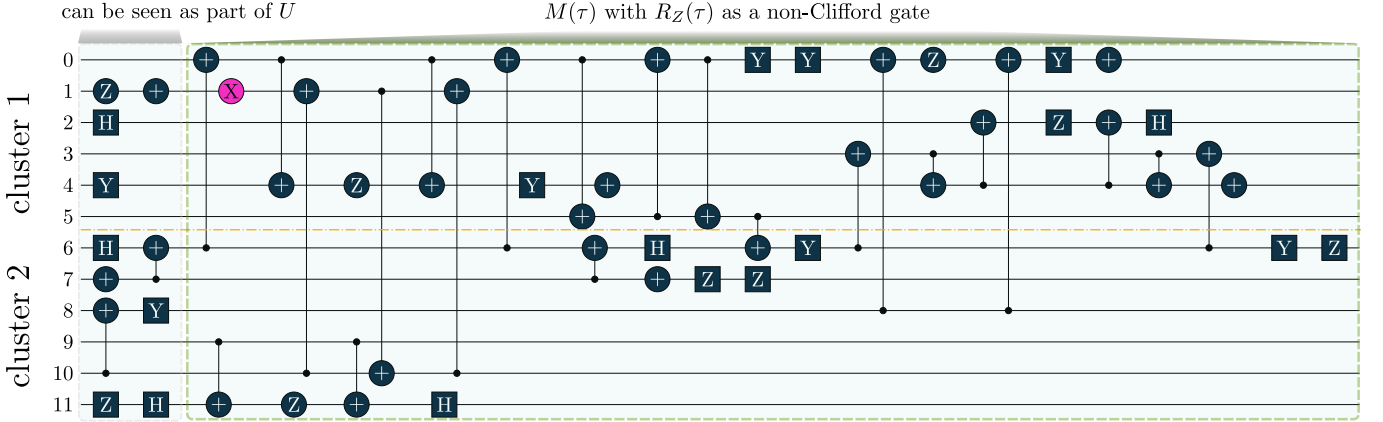


FIG. 9: Optimized circuit architecture for  $N_2$  at a bond distance of 2.0 Ångstrom; pink gates denote a parametrized gate and are thus non-Clifford gates. Note that gates in the beginning until the first gate with support beyond two clusters can technically be seen as an extension of the quantum circuit as they do not add correlation between clusters. One may choose to allow or not allow such gates.

connectivity between qubits as when reduced to individual problems on less qubits, one can use better-connected parts of the architecture only.

We explored the capabilities of Clifford and near-Clifford circuits to re-entangle a molecular wavefunction that has been enforced into the form of a product state. Within our proposed procedure, we use the energy as the only, global criterion for optimization; we deploy a genetic algorithm that mutates a set of random, initial virtual circuits using a Clifford operator pool. After suc-

cessful optimization of the Clifford circuit, we “turn on” the parameter of one one the Clifford gates in the virtual circuit to further improve the energy (while continuing to adjust the parameters in the cluster circuit). As we demonstrate, the increase in measurement cost using such near-Clifford circuits is still modest. A worthwhile direction to follow in the future would be to perform a more concise investigation of near-Clifford operations in this context, e.g. resorting to the proposed approach in Ref. [57] to assess the Hamiltonian growth.

Future work might include investigating more sophisticated genetic algorithms. Aside of cross-population mutations that enable broader exploration of the space of Clifford circuits, it would be interesting to include populations with permuted orbital ordering at the beginning of the optimization procedure. This is motivated by our observations in the case of  $\text{BeH}_2$  in Fig. 7b, where the permuted ordering is able to outperform the optimal ordering for some geometries.

Despite yielding significant improvements for  $\text{H}_2$  and  $\text{BeH}_2$ , the improvements we see by adding the non-Clifford gate is nearly negligible in the case of  $\text{N}_2$ , which suggests that one non-Clifford gate is not enough in this case. Thus further work needs to be done to explore near-Clifford circuits and in particular influence of few, specific gates on the expressibility of circuits.

## ACKNOWLEDGEMENTS

We thank Abhishek Rajput for valuable comments on the manuscript. A.A.-G. acknowledges the generous support from Google, Inc. in the form of a Google Focused Award. A.A.-G. also acknowledges support from the Canada Industrial Research Chairs Program, the Canada 150 Research Chairs and NSERC Discovery Program. This work was supported by the U.S. Department of Energy under Award No. DE-SC0019374. Resources used in preparing this research were provided, in part, by the Province of Ontario, the Government of Canada through CIFAR, and companies sponsoring the Vector Institute ([www.vectorinstitute.ai/partners](http://www.vectorinstitute.ai/partners)). P.S. and J.B. acknowledge support by the U.S. Department of Energy (DOE) through a quantum computing program sponsored by the Los Alamos National Laboratory (LANL) Information Science & Technology Institute. The research at LANL was supported by the Laboratory Directed Research and Development (LDRD) program under project number 20200056DR. L.C. was partially supported by the U.S. DOE, Office of Science, Office of Advanced Scientific Computing Research, under the Accelerated Research in Quantum Computing (ARQC) program.

## CODE AND DATA AVAILABILITY

Results and code for the Clifford-partitioning can be found at <https://github.com/philipp-q/partitioning-with-cliffords>. Furthermore code for the power method based reference methods can be found at [https://github.com/philipp-q/power\\_method\\_for\\_product\\_states](https://github.com/philipp-q/power_method_for_product_states).

## REFERENCES

- [1] A. Aspuru-Guzik, A. D. Dutoi, P. J. Love, and M. Head-Gordon, *Science* **309**, 1704 (2005).
- [2] Y. Cao, J. Romero, J. P. Olson, M. Degroote, P. D. Johnson, M. Kieferová, I. D. Kivlichan, T. Menke, B. Peropadre, N. P. Sawaya, *et al.*, *Chemical reviews* **119**, 10856 (2019).
- [3] S. McArdle, S. Endo, A. Aspuru-Guzik, S. C. Benjamin, and X. Yuan, *Reviews of Modern Physics* **92**, 015003 (2020).
- [4] A. Peruzzo, J. McClean, P. Shadbolt, M.-H. Yung, X.-Q. Zhou, P. J. Love, A. Aspuru-Guzik, and J. L. O'Brien, *Nature communications* **5**, 1 (2014).
- [5] O. Higgott, D. Wang, and S. Brierley, *Quantum* **3**, 156 (2019).
- [6] K. M. Nakanishi, K. Mitarai, and K. Fujii, *Physical Review Research* **1**, 033062 (2019).
- [7] J. R. McClean, M. E. Kimchi-Schwartz, J. Carter, and W. A. De Jong, *Physical Review A* **95**, 042308 (2017).
- [8] A. Asthana, A. Kumar, A. Vibin, H. Grimsley, Y. Zhang, L. Cincio, S. Tretiak, P. A. Dub, S. E. Economou, E. Barnes, *et al.*, *Chemical Science* (2023).
- [9] M. Cerezo, A. Arrasmith, R. Babbush, S. C. Benjamin, S. Endo, K. Fujii, J. R. McClean, K. Mitarai, X. Yuan, L. Cincio, *et al.*, *Nature Reviews Physics* **3**, 625 (2021).
- [10] J. Tilly, H. Chen, S. Cao, D. Picozzi, K. Setia, Y. Li, E. Grant, L. Wossnig, I. Runger, G. H. Booth, *et al.*, *Physics Reports* **986**, 1 (2022).
- [11] K. Bharti, A. Cervera-Lierta, T. H. Kyaw, T. Haug, S. Alperin-Lea, A. Anand, M. Degroote, H. Heimonen, J. S. Kottmann, T. Menke, *et al.*, *Reviews of Modern Physics* **94**, 015004 (2022).
- [12] A. Kandala, A. Mezzacapo, K. Temme, M. Takita, M. Brink, J. M. Chow, and J. M. Gambetta, *Nature* **549**, 242 (2017).
- [13] A. Anand, P. Schleich, S. Alperin-Lea, P. W. K. Jensen, S. Sim, M. Díaz-Tinoco, J. S. Kottmann, M. Degroote, A. F. Izmaylov, and A. Aspuru-Guzik, *Chemical Society Reviews* **51**, 1659 (2022).
- [14] P. J. Ollitrault, A. Bardi, M. Reiher, and I. Tavernelli, *Chemical science* **11**, 6842 (2020).
- [15] J. Preskill, *Quantum* **2**, 79 (2018).
- [16] Y. Zhang, L. Cincio, C. F. Negre, P. Czarnik, P. J. Coles, P. M. Anisimov, S. M. Mniszewski, S. Tretiak, and P. A. Dub, *npj Quantum Information* **8**, 96 (2022).
- [17] A. Eddins, M. Motta, T. P. Gujarati, S. Bravyi, A. Mezzacapo, C. Hadfield, and S. Sheldon, *PRX Quantum* **3**, 010309 (2022).
- [18] J. S. Kottmann and A. Aspuru-Guzik, *Phys. Rev. A* **105**, 032449 (2022).
- [19] J. S. Kottmann, P. Schleich, T. Tamayo-Mendoza, and A. Aspuru-Guzik, *The Journal of Physical Chemistry Letters* **12**, 663 (2021).
- [20] J. S. Kottmann, F. A. Bischoff, and E. F. Valeev, *The Journal of Chemical Physics* **152**, 074105 (2020).
- [21] I. G. Ryabinkin, R. A. Lang, S. N. Genin, and A. F. Izmaylov, *J. Chem. Theory Comput.* **16**, 1055 (2020).
- [22] Z.-X. Shang, M.-C. Chen, X. Yuan, C.-Y. Lu, and J.-W. Pan, *arXiv preprint arXiv:2112.07881* (2021).
- [23] D. Gottesman, *Physical Review A* **57**, 127 (1998).
- [24] D. Gottesman, *arXiv preprint quant-ph/9807006* (1998).

[25] S. Bravyi and A. Kitaev, *Physical Review A* **71**, 022316 (2005).

[26] E. Knill, D. Leibfried, R. Reichle, J. Britton, R. B. Blakestad, J. D. Jost, C. Langer, R. Ozeri, S. Seidelin, and D. J. Wineland, *Physical Review A* **77**, 012307 (2008).

[27] E. Magesan, J. M. Gambetta, and J. Emerson, *Physical review letters* **106**, 180504 (2011).

[28] J. Chen, D. Ding, C. Huang, and L. Kong, *arXiv preprint arXiv:2206.08293* (2022).

[29] K. Mitarai, Y. Suzuki, W. Mizukami, Y. O. Nakagawa, and K. Fujii, *Physical Review Research* **4**, 033012 (2022).

[30] P. Czarnik, A. Arrasmith, P. J. Coles, and L. Cincio, *Quantum* **5**, 592 (2021).

[31] M. H. Cheng, K. E. Khosla, C. N. Self, M. Lin, B. X. Li, A. C. Medina, and M. S. Kim, “Clifford circuit initialisation for variational quantum algorithms,” (2022).

[32] A. Anand, J. S. Kottmann, and A. Aspuru-Guzik, *arXiv e-prints*, arXiv (2022).

[33] G. S. Ravi, P. Gokhale, Y. Ding, W. M. Kirby, K. N. Smith, J. M. Baker, P. J. Love, H. Hoffmann, K. R. Brown, and F. T. Chong, *arXiv preprint arXiv:2202.12924* (2022).

[34] N. V. Tkachenko, J. Sud, Y. Zhang, S. Tretiak, P. M. Anisimov, A. T. Arrasmith, P. J. Coles, L. Cincio, and P. A. Dub, *PRX Quantum* **2**, 020337 (2021).

[35] J. S. Kottmann, *arXiv preprint arXiv:2207.12421* (2022).

[36] A. F. Izmaylov, T.-C. Yen, R. A. Lang, and V. Verteletskyi, *Journal of chemical theory and computation* **16**, 190 (2019).

[37] T.-C. Yen, V. Verteletskyi, and A. F. Izmaylov, *Journal of chemical theory and computation* **16**, 2400 (2020).

[38] V. Verteletskyi, T.-C. Yen, and A. F. Izmaylov, *The Journal of chemical physics* **152**, 124114 (2020).

[39] X. Bonet-Monroig, R. Babbush, and T. E. O’Brien, *Physical Review X* **10**, 031064 (2020).

[40] T.-C. Yen and A. F. Izmaylov, *PRX Quantum* **2**, 040320 (2021).

[41] W. J. Huggins, J. R. McClean, N. C. Rubin, Z. Jiang, N. Wiebe, K. B. Whaley, and R. Babbush, *npj Quantum Information* **7**, 1 (2021).

[42] S. Sim, P. D. Johnson, and A. Aspuru-Guzik, *Advanced Quantum Technologies* **2**, 1900070 (2019).

[43] J. S. Kottmann, A. Anand, and A. Aspuru-Guzik, *Chemical Science* **12**, 3497 (2021).

[44] A. F. Izmaylov, R. A. Lang, and T.-C. Yen, *Physical Review A* **104**, 062443 (2021).

[45] D. Wierichs, J. Izaac, C. Wang, and C. Y.-Y. Lin, *Quantum* **6**, 677 (2022).

[46] O. Kyriienko and V. E. Elfving, *Physical Review A* **104**, 052417 (2021).

[47] M. Schuld, V. Bergholm, C. Gogolin, J. Izaac, and N. Killoran, *Physical Review A* **99**, 032331 (2019).

[48] I. G. Ryabinkin, T.-C. Yen, S. N. Genin, and A. F. Izmaylov, *J. Chem. Theory Comput.* **14**, 6317 (2018).

[49] R. Xia and S. Kais, *Quantum Science and Technology* **6**, 015001 (2020).

[50] I. O. Sokolov, P. K. Barkoutsos, P. J. Ollitrault, D. Greenberg, J. Rice, M. Pistoia, and I. Tavernelli, *The Journal of chemical physics* **152**, 124107 (2020).

[51] W. Mizukami, K. Mitarai, Y. O. Nakagawa, T. Yamamoto, T. Yan, and Y.-y. Ohnishi, *Phys. Rev. Research* **2**, 033421 (2020).

[52] S. Yalouz, B. Senjean, J. Günther, F. Buda, T. E. O’Brien, and L. Visscher, *Quantum Science and Technology* **6**, 024004 (2021).

[53] J. Biamonte, *Physical Review A* **103**, L030401 (2021).

[54] J. Tolar, in *Journal of Physics: Conference Series*, Vol. 1071 (IOP Publishing, 2018) p. 012022.

[55] R. Jozsa and M. V. d. Nest, *arXiv preprint arXiv:1305.6190* (2013).

[56] R. A. Lang, I. G. Ryabinkin, and A. F. Izmaylov, *Journal of Chemical Theory and Computation* **17**, 66 (2020).

[57] R. A. Lang, A. Ganeshram, and A. F. Izmaylov, *arXiv preprint arXiv:2210.03875* (2022).

[58] H. R. Grimsley, S. E. Economou, E. Barnes, and N. J. Mayhall, *Nat. commun.* **10**, 1 (2019).

[59] H. L. Tang, V. Shkolnikov, G. S. Barron, H. R. Grimsley, N. J. Mayhall, E. Barnes, and S. E. Economou, *PRX Quantum* **2**, 020310 (2021).

[60] H. G. Burton, D. Marti-Dafcik, D. P. Tew, and D. J. Wales, *arXiv preprint arXiv:2207.00085* (2022).

[61] A. Fagan and R. Duncan, *Electronic Proceedings in Theoretical Computer Science* **287**, 85 (2019).

[62] J. Richter, O. Lunt, and A. Pal, *arXiv preprint arXiv:2205.06309* (2022).

[63] J. S. Kottmann, S. Alperin-Lea, T. Tamayo-Mendoza, A. Cervera-Lierta, C. Lavigne, T.-C. Yen, V. Verteletskyi, P. Schleich, A. Anand, M. Degroote, et al., *Quantum Science and Technology* **6**, 024009 (2021).

[64] Y. Suzuki, Y. Kawase, Y. Masumura, Y. Hiraga, M. Nakadai, J. Chen, K. M. Nakanishi, K. Mitarai, R. Imai, S. Tamiya, et al., *Quantum* **5**, 559 (2021).

[65] R. J. Harrison, G. Beylkin, F. A. Bischoff, J. A. Calvin, G. I. Fann, J. Fosso-Tande, D. Galindo, J. R. Hammond, R. Hartman-Baker, J. C. Hill, et al., *SIAM Journal on Scientific Computing* **38**, S123 (2016).

[66] R. J. Harrison, G. I. Fann, T. Yanai, Z. Gan, and G. Beylkin, *The Journal of chemical physics* **121**, 11587 (2004).

[67] F. A. Bischoff, *The Journal of chemical physics* **141**, 184105 (2014).

[68] J. R. McClean, N. C. Rubin, K. J. Sung, I. D. Kivlichan, X. Bonet-Monroig, Y. Cao, C. Dai, E. S. Fried, C. Gidney, B. Gimby, et al., *Quantum Science and Technology* **5**, 034014 (2020).

[69] D. G. Smith, L. A. Burns, A. C. Simmonett, R. M. Parish, M. C. Schieber, R. Galvelis, P. Kraus, H. Kruse, R. Di Remigio, A. Alenaizan, et al., *The Journal of chemical physics* **152**, 184108 (2020).

[70] P. Schleich, J. S. Kottmann, and A. Aspuru-Guzik, *Physical Chemistry Chemical Physics* **24**, 13550 (2022).

[71] R. Orús, *Annals of physics* **349**, 117 (2014).

## Appendix A: Product-state enforcing reference method

Given a fermionic Hamiltonian  $H_{\text{ferm}}$ , we use a quantum-chemical encoding [2, 3] to obtain a qubit Hamiltonian  $H_{\text{qc}}$  as a linear combination of Pauli strings. Our code for the following method is available at [https://github.com/phillipp-q/power\\_method\\_for\\_product\\_states](https://github.com/phillipp-q/power_method_for_product_states).

Then, we use a generic wavefunction as a tensor over the qubit space, assuming a product state. For the sake of clarity, we will only show the case of two clusters and note that this can be arbitrarily extended. Then, for  $N_q$  qubits, this gives  $|\psi\rangle \in \mathbb{C}^{2^{N_q/2}} \otimes \mathbb{C}^{2^{N_q/2}}$ . We use a random, initial wavefunction factorized over subsystems  $A, B$  with uniformly sampled and normalized coefficients in a Pauli basis.

Further, we define the reduced Hamiltonians of the subsystems  $A, B$  as

$$H_A = \text{Tr}_B(H) = \langle(\cdot)\psi_B|H|(\cdot)\psi_B\rangle \quad (\text{A1})$$

$$H_B = \text{Tr}_A(H) = \langle\psi_A(\cdot)|H|\psi_A(\cdot)\rangle, \quad (\text{A2})$$

where  $H_A$  is obtained by tracing out all subsystems except for  $A$ ; see also Fig. 10.

To find the ground-state, we perform the following power method-type iterations using the reduced Hamiltonians for each systems, where  $|\psi^{(i)}\rangle = |\psi_A^{(i)}\rangle \otimes |\psi_B^{(i)}\rangle$ :

$$|\psi_A^{(i+1)}\rangle = H_A |\psi_A^{(i)}\rangle - \gamma |\psi_A^{(i)}\rangle \quad (\text{A3})$$

$$|\psi_B^{(i+1)}\rangle = H_B |\psi_B^{(i)}\rangle - \gamma |\psi_B^{(i)}\rangle. \quad (\text{A4})$$

For our computations, we use  $\gamma = 1$  and use a convergence criterion of

$$|E^{(i)} - E^{(i+1)}| \leq \text{TOL} \quad \text{where} \quad E^{(i)} = \langle\psi_A^{(i)}\psi_B^{(i)}|H|\psi_A^{(i)}\psi_B^{(i)}\rangle, \quad (\text{A5})$$

with  $\text{TOL} = 10^{-5}$  milli-Hartree. We note that we keep the wavevectors as full vectors. For computationally more involved experiments than presented in this work, one could think of a representation using tensor network methods [71].

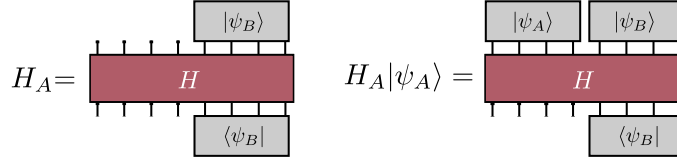


FIG. 10: Hamiltonian that has been reduced over subspace  $B$  and now acts only on subspace  $A$ .

## Appendix B: Examples for optimized circuits

Below, we show some exemplary circuits for each molecule that showed higher/lower performance; this data is also part of our github repository at <https://github.com/philipp-q/partitioning-with-cliffords>. We note that we only show the near-Clifford version with the best-performing non-Clifford gate (pink) as the respective Clifford circuit is simply given by a fixed parametrization. We provide the optimal angles in Table II, where we notice that for nitrogen, two of the computations yield (effectively) Clifford circuits. Beyond that, we note that in almost every case except for once, a parametrized  $Z$  rotation yields the best configuration.

	Geometry/Å	Angle/rad	Rotation gate
BeH <sub>2</sub>	1.0	-0.00466767	$R_Z$
	3.0	0.00155535	$R_Z$
N <sub>2</sub>	3.0	– (effectively Clifford)	$R_Z$
	1.5	– (Clifford)	–
	2.25	0.03207715	$R_Z$
H <sub>2</sub>	1.4	$2.1953 \cdot 10^{-5}$	$R_X$
	2.8	0.00329714	$R_Z$

TABLE II: Angles for non-Clifford gates in example circuits.

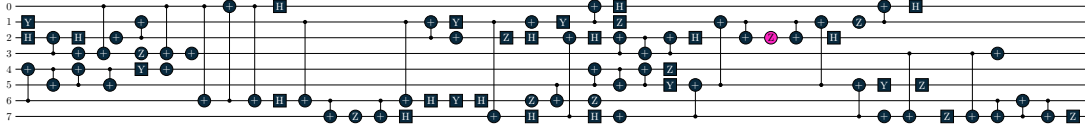


FIG. 11: Better-performing near-Clifford circuit for BeH<sub>2</sub> at a bond distance of 1.0 Ångstrom.

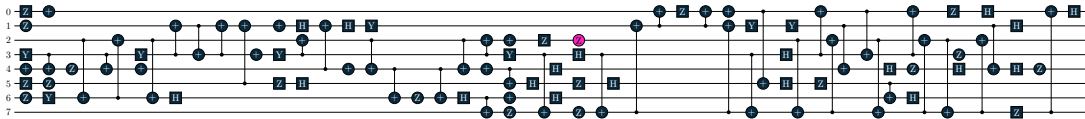


FIG. 12: Near-Clifford circuit for BeH<sub>2</sub> at 3.0 Ångstrom; for BeH<sub>2</sub>, the improvement is rather constant and less fluctuating than for N<sub>2</sub>.

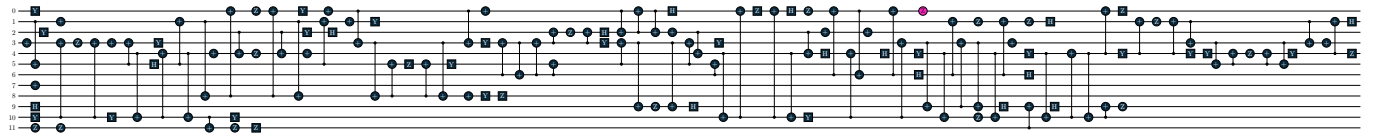


FIG. 13: Near-Clifford circuit for N<sub>2</sub> at bond distance 3.0; here, substantial improvement beyond the reference and the SPA is noticed (compare to Fig. 6), although the final, optimal circuit turned out to be effectively Clifford (see Table II).

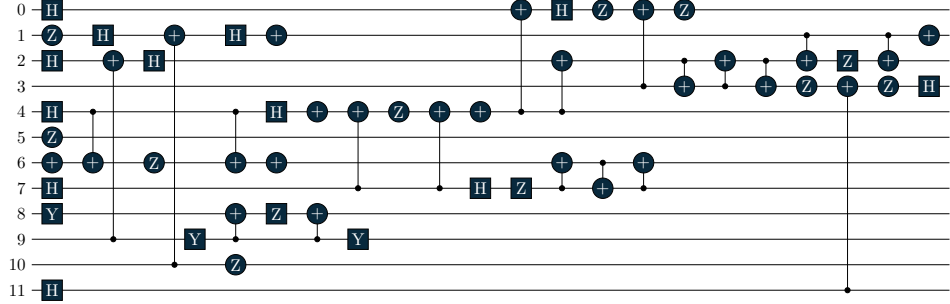


FIG. 14: Poorly performing near-Clifford optimization for  $N_2$  at bond distance 1.5; here, when attempting to parametrize non-Clifford gates, no improvement could have been made out, so the result remains a Clifford circuit.

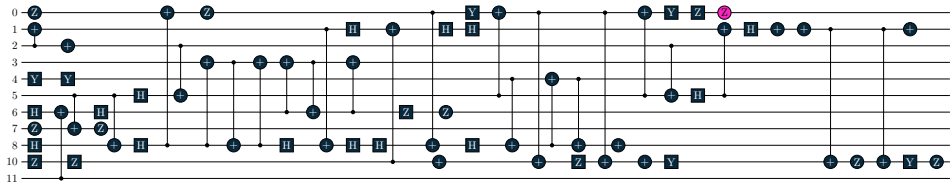


FIG. 15: Well-performing near-Clifford optimization for  $N_2$  at bond distance 2.25; for this configuration, no actions have been performed on qubit 9.

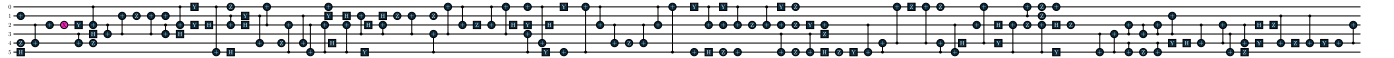


FIG. 16: Near-Clifford circuit for  $H_2$  at bond distance 1.4; adding and optimizing a non-Clifford gate improves error by roughly an order of magnitude here.

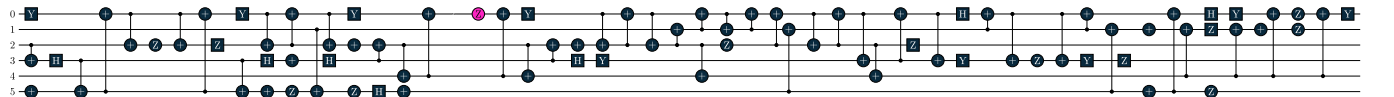


FIG. 17: Near-Clifford circuit for  $H_2$  at bond distance 2.8; little improvement by adding a non-Clifford gate was observed for this configuration.